PROCEEDINGS OF SPIE

SPIEDigitalLibrary.org/conference-proceedings-of-spie

Evidence that evaporated Al/AlF3 bilayer thin films stored in a 327 K oven for over 2500 hours have not degraded

Kenan Fronk, David Allred

Kenan Fronk, David D. Allred, "Evidence that evaporated Al/AlF3 bilayer thin films stored in a 327 K oven for over 2500 hours have not degraded ," Proc. SPIE 12181, Space Telescopes and Instrumentation 2022: Ultraviolet to Gamma Ray, 121813A (31 August 2022); doi: 10.1117/12.2630711

SPIE.

Event: SPIE Astronomical Telescopes + Instrumentation, 2022, Montréal, Québec, Canada

Downloaded From: https://www.spiedigitallibrary.org/conference-proceedings-of-spie on 28 Dec 2022 Terms of Use: https://www.spiedigitallibrary.org/terms-of-use

Evidence that evaporated Al/AlF_3 bilayer thin films stored in a 327 K oven for over 2500 hours have not degraded

Kenan Fronk[1ab] and David D. Allred[a]

[a]Dept. of Physics and Astronomy, Brigham Young University, Provo, UT USA 84602, [b]currently, Dept. of Metallurgical and Materials Engineering, University of Alabama, Tuscaloosa, AL USA 35487

ABSTRACT

Four evaporated, thin-film Al samples protected by a thin (29±2 nm) aluminum fluoride (AlF_3) overcoat stored in dry (dew point 276K), 327 K air over a period of 2500 hours exhibited no significant changes in the thickness of the protective AlF_3 layer nor growth in aluminum oxide as observed by variable-angled, spectroscopic ellipsometry. Two of the samples had AlF_3 evaporated at T>200°C, two without substrate heating. No difference in aging was noted amongst the samples. Since many months may elapse between fabrication and launch of the completed observatory, this result contributes to understanding the boundaries in temperature and humidity separating negligible changes in fluoride-containing optical components from unacceptable degradation. While negligible changes in thicknesses were observed, there were changes in the ellipsometric data, psi and delta, with time. In this study, we also present our use of an effective medium approximation model in understanding changes in the fluoride layer with aging. The observed changes in SE parameters are here interpreted as changes in void fraction, though the presence of some water was not ruled out. Apparent void fraction fell by a factor of two by the end of the 2500 hours. The decreasing void fraction suggests that the films might be becoming more compact with time. Other surface sensitive techniques such as AFM are needed to narrow down possible explanations for observed changes.

Keywords: thin films, mirrors, ultraviolet, aluminum, aluminum fluoride, storage, atomic force microscopy, spectroscopic ellipsometry

1. INTRODUCTION

The performance of telescopes depend on the reflectance of the mirrors being used. The thin-film mirror coatings used in telescopes for broadband applications, such as far UV (FUV) through IR, need to be made from a material that provides high reflectance for both high and low energy light. Aluminum (Al) is the best broadband, high reflectance material. Calculations using optical constants[1] show that bare aluminum could provide >85% normal-incidence reflectance up to 14 eV (>89 nm) and >90% reflectance over most of the 0-14 eV range. However, as aluminum oxidizes, its FUV reflectance drops significantly. Calculations show a significant drop in FUV reflectance with minor oxidation. For example, 1 nm of Al_2O_3 should cause a 20% drop in normal-incidents reflectance.[2] Unfortunately, aluminum is prone to oxidation, even under high-vacuum conditions[3]. To combat oxidation, a fluoride capping layer is deposited immediately after the Al deposition and without breaking vacuum to help seal the aluminum surface.[4,5,6] Metallic fluorides with high band gaps, such as lithium fluoride (LiF) are desirable capping layers.[7] However, LiF is hygroscopic and degrades in high relative humidity.[8] Instead, magnesium fluoride (MgF_2) has been used because it is more stable. It is less susceptible to humidity than LiF.[6] Recently, due to the low FUV absorption of aluminum fluoride (AlF_3) it is also being investigated as a capping layer.[9–11] AlF_3 is not as resistant to water as is MgF_2. In fact, the room-temperature maximum molar solubility of AlF_3 is more similar to that of LiF. (0.08M vs. 0.05M). Whereas, MgF_2 maximum molar solubility is 0.002 M. Thus, our study may also be useful for understanding Al capped with LiF films. The purpose of this study was to investigate how storing AlF_3 capped Al films in an environment similar to a hot storage room would affect the capping layer and the oxidation of the capped aluminum.

Despite the longstanding usage of metallic fluorides as capping layers, there remain questions as to how these protective layers change over time. High reflectance, fluoride-capped Al mirrors are often stored for months or years before being

[1] *fronkkenan@gmail.com; phone 1 714-345-5462

Space Telescopes and Instrumentation 2022: Ultraviolet to Gamma Ray, edited by Jan-Willem A. den Herder, Shouleh Nikzad, Kazuhiro Nakazawa, Proc. of SPIE Vol. 12181, 121813A · © 2022 SPIE · 0277-786X · doi: 10.1117/12.2630711

Downloaded From: https://www.spiedigitallibrary.org/conference-proceedings-of-spie on 28 Dec 2022
Terms of Use: https://www.spiedigitallibrary.org/terms-of-use

implemented in optical applications. During these times, it is imperative that there is no significant swelling, shrinking, or recrystallization of the capping layer since these could allow the Al to begin oxidizing, diminishing the mirror reflectance. Thus, the need to better understand under what conditions AlF_3 capping layers change and how the underlying layer oxidizes.

We deposited four AlF_3 on Al thin film samples and placed them in an oven to simulate a hot storage room in summer. Two were deposited on room-temperature substrates, two on heated substrates. The samples were periodically measured using ellipsometry to gauge the apparent thicknesses of the Al, AlF_3 and the formation of Al oxide over time. This study shows that storing AlF_3 on Al bilayer films in a 327 K dry environment causes no significant changes in layer thicknesses and no increase in oxide. In this way, the thin-film mirror and telescope community will be able to better understand how temperature affects mirrors when they are in storage before use. The next section details sample preparation, characterization and storage conditions.

2. METHODS AND ANALYSIS

2.1 Deposition of Al and AlF_3

Four AlF_3 on Al bilayer films were deposited on a 300 nm silicon nitride (Si_3N_4) coated Si wafer using a Veeco® thermal evaporator for this study of the aging of AlF_3-protected mirror coatings. In addition, a single layer of AlF_3 on Si was prepared, measured and its aging studied. The evaporator had three independent, resistance-heated evaporation sources with two independent power supplies, so that Al and AlF_3 could be deposited immediately one after the other without breaking vacuum and with minimal time between layer depositions. Aluminum was evaporated from a tungsten coil. The chunks of aluminum fluoride were placed in a standard (RD Mathis) molybdenum evaporation boat.

An Inficon quartz-crystal thickness monitor (QCM) provided the feedback to control film thickness and deposition rates. An electronic oscillator drives the quartz crystal and monitors changes in its frequency as material is deposited on it, which allowed for a quick and precise way to measure deposition thickness in situ[2]. Two separate manual shutters were used in the deposition processes to control film thickness. The top shutter was placed immediately below the



Figure 1: The apparatus used to deposit Al and AlF_3 on the Si/Si_3N_4 substrate wafers. Note the Al (coil to left), AlF_3 (Mo boat to right) and the flag-shaped, rotatable shutter between the two evaporation sources. Shutter is used to control which evaporant reaches the samples. At this position it partially blocks the Al source. It would be rotated further to left for fluoride deposition and 90° to the right for Al deposition. The top shutter is not shown.

[2] More information on Inficon QCM crystals can be found at infinicon.com.

Downloaded From: https://www.spiedigitallibrary.org/conference-proceedings-of-spie on 28 Dec 2022
Terms of Use: https://www.spiedigitallibrary.org/terms-of-use

substrates mounted on the sample platen- closed, it covered the substrates so that they were out of the line-of-sight of all evaporation sources; opened, and evaporated molecules could reach the substrates from whatever sources were hot enough and were not covered by the lower shutter. The lower shutter is located between two deposition sources: Al and AlF_3, flag shaped, its rotation axis is horizontal and lies between the two sources as shown in Fig.1. The axis is attached to a rotational feedthrough. Tilting the flag to the right covered the AlF_3 source but left the Al source line-of-sight access to the chamber. Tilted sufficiently to the left, it covered the Al source, but gave the AlF_3 molecules evaporating from that source line-of-sight access to the chamber. Thus, both sources could be hot, but only one at a time would be coating the substrates. This had the advantage that one could switch immediately from depositing Al to depositing AlF_3. Doing this minimized to a couple of seconds the time the freshly evaporated Al films were bare. This is important since even under high vacuum conditions the far ultraviolet (FUV) reflectance of a freshly evaporated Al surface begins to fall in seconds as it begins to oxidize.[3]

Turning now to the substrate holder, the 40-cm-diameter sample platen was drilled in a grid pattern like an optical breadboard with threaded holes every inch. It sat about 37 cm above the evaporation sources covering the top of the bell jar when it was in place. It is long known that many fluorides such as MgF_2 and LiF have superior far UV optical properties when deposited at elevated temperatures[9,10,12–19]. Prior research shows that the optical properties of evaporated AlF_3 improve significantly when deposited on heated substrates[16,20] above 200°C, so a heater was constructed, and half the samples were prepared on a heated substrate. The lab-built substrate heater consisted of a pair of 12V resistance heaters in an aluminum case with rectangular dimensions of 26 mm x 60 mm place side-by-side. The heater was formally isolated from the sample platen though attached to it. The heater temperature used to heat the samples was about 510 ± 15 K. The samples were in physical contact with the heater.

For the AlF_3 on Al samples, approximately 30 mm by 30 mm squares were cleaved from a 200 mm diameter Si (100) wafer coated with a nominal 300 nm of CVD Si_3N_4. The CVD Si_3N_4 dielectric layer on the substrate is referred to as the interference layer (IL) and via spectroscopic ellipsometry facilitated measuring the thickness of the aluminum layer and the oxidation of the aluminum if the layer is semitransparent.[19,21–23] In this study, we deliberately chose to use ultrathin, that is, semitransparent aluminum to take advantage of interference enhancement[19,24] to monitor any changes in the aluminum as well as the aluminum fluoride. Thus, the FUV reflectance of these samples cannot be compared with mirrors prepared for high FUV reflectance. In preparing the four samples, half of the samples were fixed directly to the 40-cm-diameter sample platen, while the remainder two were fixed to a heater mounted directly to the platen stage. During AlF_3 deposition, the heater had a nominal temperature of 475 ± 10 K. The Al was evaporated at a rate of 0.7 nm/sec and the AlF_3 was evaporated at a rate of 0.15 nm/sec. Both the Al and AlF_3 were deposited sequentially without breaking vacuum. The system pressure was $4x10^{-4}$ Pa prior to evaporation. Deposition of both Al and AlF_3 took about four minutes. The nominal thickness of the Al and AlF_3 cap were respectively 20 and 30 nm. Table 1 has measurements.

2.2 Characterization

2.2.1 Ellipsometric Characterization

We determined the thicknesses of the thin-film mirror samples in this study using variable-angle, spectroscopic ellipsometry (VASE). We chose ellipsometry as our method for tracking the thicknesses of the films because measurements can be made easily, quickly and in air.[19,21–23] The models used for each layer and the procedure used to obtain reliable numbers are discussed below and in reference 2. Since this our first report of using an EMA for modeling the fluoride barrier useful for VUV mirrors, we discuss this in detail in the results section.

Immediately after the initial deposition, the samples were removed from the deposition chamber and measured with a J.A. Woollam M-2000D ellipsometer (J.A. Woollam Company, Lincoln, ME, USA) over the wavelength range of 190-1688 nm and at several angles. This measurement provided the as-deposited thicknesses of the layers. Ellipsometric reflectance data was analyzed using the CompleteEASE software provided by the J.A. Woollam Company. The model used for analyzing the data in CompleteEASE is based on the layers seen in the Fig. 2. Many of the initial layer parameters used in the first fit were based on the CompleteEASE data and the rest were created and fit from previous samples as discussed below. In order to obtain reliable and quantitative results on changes in the evaporated layers, it was critical that the substrate and the bottom three layers be measured and adequately modeled prior to depositing the aluminum/AlF_3 layers. That is, the layers starting at the bottom with the substrate (Si plus layers one through three) were analyzed independently and their optical constants and thicknesses fixed before the next layer or set of layers is analyzed. (In practice, the thicknesses of layers one and three are fixed, and the thickness of layer 2 is fixed for all

Downloaded From: https://www.spiedigitallibrary.org/conference-proceedings-of-spie on 28 Dec 2022
Terms of Use: https://www.spiedigitallibrary.org/terms-of-use

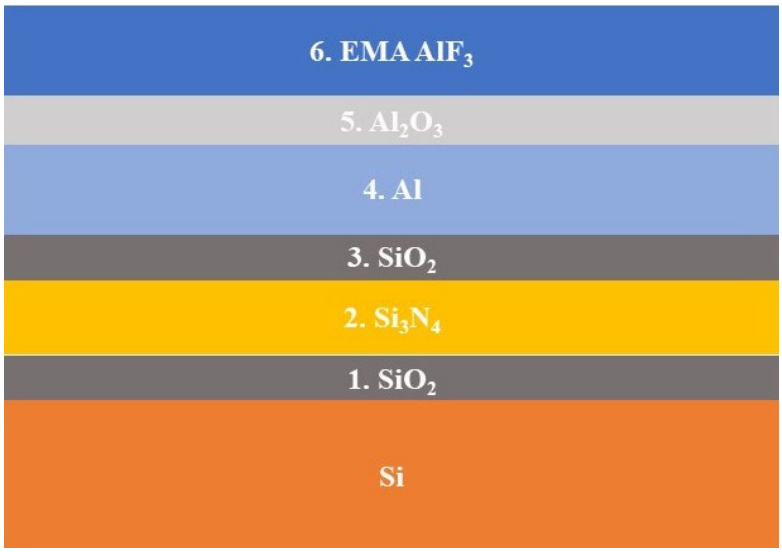


Figure 2. Representation of the optical stack of the samples created. Layer 6 is the AlF_3 capping layer and is modeled with an effective medium approximation (EMA). Modeling layer six with an EMA allows us to include secondary constituents like voids and water in a primary matrix of AlF_3. Layer thicknesses are not shown to scale.

measurements throughout the storage studies.) Only in this way could the thicknesses of the top layers be adequately fit. It is absolutely crucial that discipline is followed. The fitting process will produce unphysical results, if the parameters of layers that are already known are allowed to vary while the top layers are being fit. This is discussed in more detail in reference 19.

There were three dielectrics layers that we created models for: Si_3N_4, Al_2O_3, and AlF_3. Layer 2 is chemical vapor deposited (CVD) Si_3N_4. It is amorphous, not crystalline, and thus possesses different optical constants than recorded for crystalline nitride. We had previously found that the optical constants of Si_3N_4 could be parameterized successfully as a Tauc-Lorentz oscillator plus a Gaussian oscillator located at about 6 eV.[19] The same prior study showed that there was a thin SiO_2 layer on the surface of the Si_3N_4. Its thickness was between 1 and 2 nm, and we fixed the thickness of layer 3 at 1 nm in our model. We used optical constant data from Herzinger[25] as stored in the CompleteEASE® database for layers 1,3 and substrate. Layer 5 is the second dielectric, Al_2O_3. It is the thinnest of the layers in the multilayer, since, if it is there at all, it is not deposited but grows from the gradual oxidation of the Al layer. Al_2O_3 was parameterized as a Cauchy layer, with parameters fit using previous studies from our group. Layer 6 is the deposited AlF_3 capping layer. As the samples aged, we observed that the fluoride layers could appear to change in apparent thickness and optical constants. Apparent increase in thickness was previously observed in our group's previous studies of MgF_2 on Al layers.[19,21,23] However, the MgF_2 layers studied there were less than 10 nm and, at the time, changes in ellipsometric data with time were attributable to aluminum oxidation. The present study is a further, more difficult step since the AlF_3 as well as the Al beneath it can change with time. A useful way to make sense of the observation that the AlF_3 layer is changing is to model this top dielectric layer as a porous AlF_3 with bulk-like constants. These could be filled with water, thought to condense via capillary action from the air in the pores. The application of capillary theory to fluoride thin films is discussed more fully elsewhere in these proceedings.[26] In this study, the AlF_3 layer was modeled by using a Bruggeman effective medium approximation (EMA) layer, with the primary material being AlF_3 and with vacuum (void) and water secondary and tertiary components. We considered the void and water to be the most important minor constituents in the primary AlF_3 matrix because of the native roughness and porosity of evaporated thin films and AlF_3's affinity for water. The evaporated AlF_3 optical constants had been measured previously and were fit using a Sellmeier model. This material was then used in the EMA layer for the samples deposited at room temperature. Another AlF_3 Sellmeier model with different fit parameters was used in the EMA layer for samples deposited on the heater, as it is known in the case of some fluorides the optical constants more closely resemble the bulk constants.[13]

Thin-film metal layers such as the Al (layer 4) need to be treated differently than dielectrics because of their free electrons. The Al layer was modeled as the sum of four Gaussian oscillators with a UV pole. UV poles are Lorentz oscillators with zero broadening that remain outside the spectral range being fit. The oscillator at zero eV corresponds to

Downloaded From: https://www.spiedigitallibrary.org/conference-proceedings-of-spie on 28 Dec 2022
Terms of Use: https://www.spiedigitallibrary.org/terms-of-use

Table 1 : The apparent layer thicknesses in nanometers for each of the four samples measured shortly after deposition. The numbers of each row coordinate with Fig.3

Sample	Room Temperature (RT) Substrate 1	Room Temperature (RT) Substrate 2	Heater Temperature (HT) Substrate 1	Heater Temperature (HT) Substrate 2
Roughness	2.00	1.86	1.88	2.21
6. EMA AlF_3	26.78	31.25	29.31	26.84
5. Al_2O_3	0.09	0.09	0.05	0.11
4. Al	19.9	19.9	23.6	23.1
2. Si_3N_4	306.35	304.8	301.1	298.1

the free-electron (Drude) contribution to aluminum's conductivity. It is known that the intensity and breadth of this oscillator varies with deposition conditions such as impurity concentration and especially with film thickness.[19,27] The oscillator parameters had been fixed from the study of an aluminum thin film of a similar thickness in a prior study. We used the same aluminum model for each sample, not adjusting the parameters values even as the sample aged. It should be noted that this approach does not guarantee that oxygen was not incorporated in the field as it was deposited. It merely permits one to determine if the aluminum changes over the course of the study. The optical effect of impurities spread uniformly in the film are folded into the aluminum's optical constants when a material's optical parameters are fit. Aluminum has grain boundaries and potentially oxygen could penetrate along these, oxidizing the film's interior over the course of the study. We investigated this possibility by replacing layer 4 with a three-component EMA layer composed of Al with voids and aluminum oxide as the minor components. We found, however, that the data fit in this way always showed an absence of voids or oxide. Thus, in fitting the ellipsometric data reported here, we used an aluminum model as described above. Fitting aluminum constants is discussed in more detail in reference 19.

Multiple sample analysis (MSA) was used in this study. MSA allows for the fitting of specified parameters for individual samples in a data set or fitting a parameter to a single value common across the data set. It is an effective tool for finding trends such as the aging of a single sample that would be harder to see if each set was analyzed sample-by-sample.[19,28,29] MSA was used to better determine the layer optical constants of both Al and AlF_3 since the optical qualities of the layers are dependent, in part, on how the samples were deposited. When fitting for the AlF_3 layer, MSA was used to calculate Sellmeier model parameters for both room-temperature deposited and heated-substrate deposited AlF_3. The parameters of the two Sellmeier models were then averaged to produce a reasonable AlF_3 that could be used for both.

2.2.2 AFM Characterization

To constrain surface roughness in the ellipsometric models, the samples were measured using atomic force microscopy (AFM). A 10 by 10 micron area was selected on each sample and then scanned three times in succession. The RMS roughnesses from the three scans for each sample were then averaged. It was observed that there was no significant difference between the roughnesses of the capping layer of the various samples. Fixing sample roughness reduces the number of free parameters in the models. Table 1 shows the initial apparent thicknesses for each sample created.

2.3 Storage in 327K oven

After initial reflectance measurements on the ellipsometer, the samples were placed in an oven at 327 K ± 10K to simulate a hot storage room. The dew point of the air was noted (276 K), but no attempt was made to control the humidity. Samples were taken out periodically, measured via ellipsometry and in some cases AFM, and then returned to the oven over the course of about 2500 hours. The average time for removing, measuring, and returning the samples to the oven was an hour. There were also several power outages that resulted in the oven cooling for brief intervals.

Downloaded From: https://www.spiedigitallibrary.org/conference-proceedings-of-spie on 28 Dec 2022
Terms of Use: https://www.spiedigitallibrary.org/terms-of-use

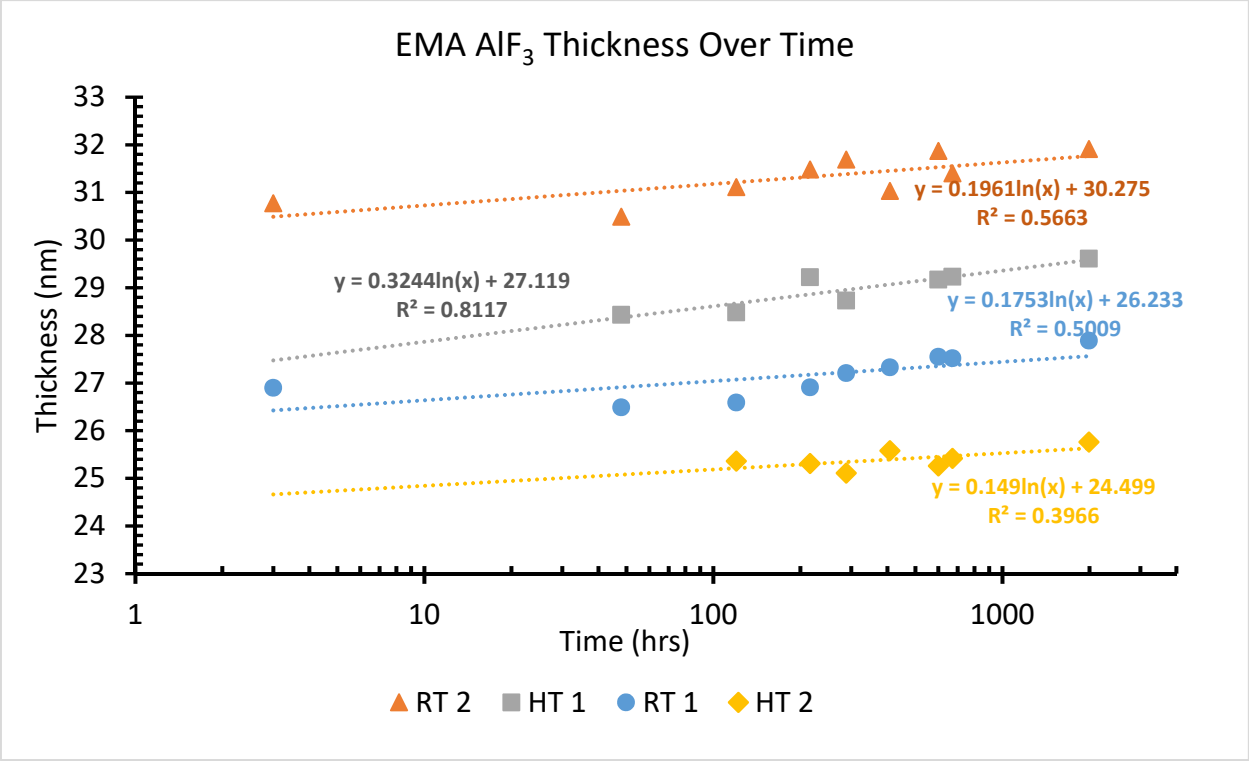


Figure 3. The apparent thicknesses of the EMA-AlF_3 layer in each sample as a function of time in the oven. The secondary constituents of the EMA layer are water and void. Trend lines with their equations and R^2 values are included.

3. Results and Discussion

3.1 Initial fit before layer parameter optimization

The first fit of the EMA AlF_3 layer is shown below in Fig. 3. Fig. 3 led us to think at first that there was significant growth in the capping layer as the time in the oven increased. However, upon reviewing the different percent values of the secondary constituents, we realized that the changes needed to be made in our fitting model.

3.2 Difficulties with the EMA model

3.2.1 Water as a secondary constituent

As discussed before, the AlF_3 was modeled by an EMA layer with AlF_3 as the primary constituent and void and water as the minor constituents. Fig. 3 above shows that according to this model, each of the samples' AlF_3 thicknesses gradually increased over time. Fig. 4 shows the water percentage in the AlF_3. For all samples this started at zero, gradually increasing to about 20-30%. We doubted the high percentage of water constituent, because it implies that the amount of AlF_3 decreased with time. This is not reasonable. To determine if the amount of water in the layer was correct, one hot sample and one cold sample was placed on a heater and held at high vacuum for 3 days. We anticipated

Downloaded From: https://www.spiedigitallibrary.org/conference-proceedings-of-spie on 28 Dec 2022
Terms of Use: https://www.spiedigitallibrary.org/terms-of-use

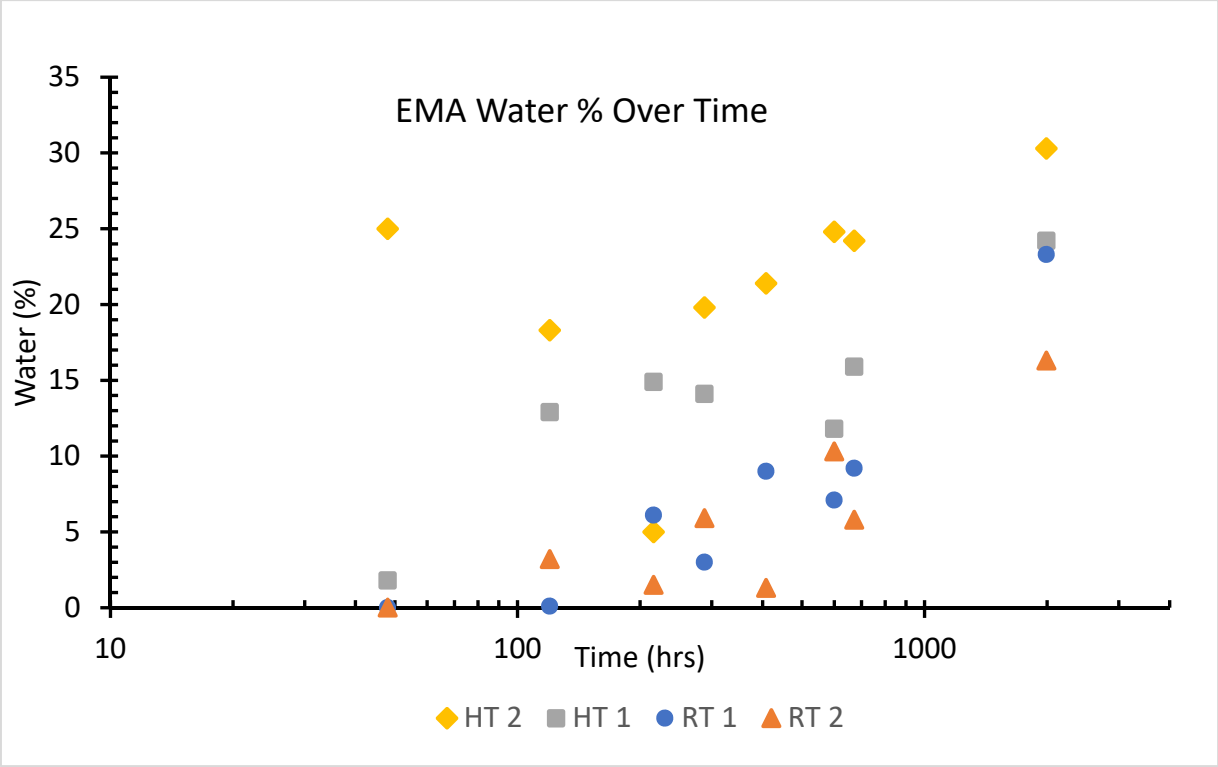


Figure 4. The constituent "water" percent for the samples vs. time in oven. If these values for water content were true, AlF_3 would be vanishing.

that some or all of the water would evaporate. The samples were measured one immediately after removal from the heater and the vacuum. That the "water" percentage did not change noticeably gave evidence that the model of substantial water in aged films was incorrect. Thus, the "water" was removed as a minor constituent while voids were retained as the minor constituent in the AlF_3-EMA layer.

3.2.1 Voids as the only minor constituent and new Al parameters yield an adequate fit

It is a safe assertion that voids would be present in the as-deposited AlF_3 layer, since this is the usual case for evaporated dielectric films. Fig. 5 shows the fitted void percentage as a function of time for each samples with the two-component EMA AlF_3-void model. The void percentage is seen to decrease with time, which is something of a mystery. The next step was to fit the parameters for the aluminum optical model. The fitting parameters for all other layers are discussed in detail elsewhere were not allowed to vary for the fit of the Al parameters. Fig. 6 shows the thickness of the AlF_3 layer for each of the four samples as calculated by this fit as a function of time enough in oven. It should be noted that for no sample was there a significant change in the thickness of the AlF_3 capping layer over the 2500 hours. In fact, the thickness of two of the four samples were best fit as not varying with time. Their thickness is constant.

3.3 Root Mean Squared Error shows the fit is good

The primary means by which we measured goodness of fit for the samples was by using "Root Mean Squared Error" (RMSE). With the CompleteEASE software, a RMSE is provided with every analyzed data set. In brief, the RMSE is a measure of differences between the measured data and model generated data over the wavelength range. An ideal model fit according to the equation used in CompleteEASE is around 1. However, with data that shows significant interference fringes RMSE will be higher. Fig. 7 shows the RMSEs for fits of all four samples as a function of time in oven. No significant trend in the RMSEs over time is apparent. This may mean that the optical model has no bias for fresh over aged samples, or vice versa. The RMSE for each sample over the duration is about 3, indicating that the computational model provides an adequate fit of the experimental data. Multilayer thin-film stacks like the ones in this study are

Downloaded From: https://www.spiedigitallibrary.org/conference-proceedings-of-spie on 28 Dec 2022
Terms of Use: https://www.spiedigitallibrary.org/terms-of-use

difficult to model and an RSME near 3 is not uncommon with the data as interference fringes. However, it may be possible to lower the RMSE by creating more complete models and better understanding the aging processes.

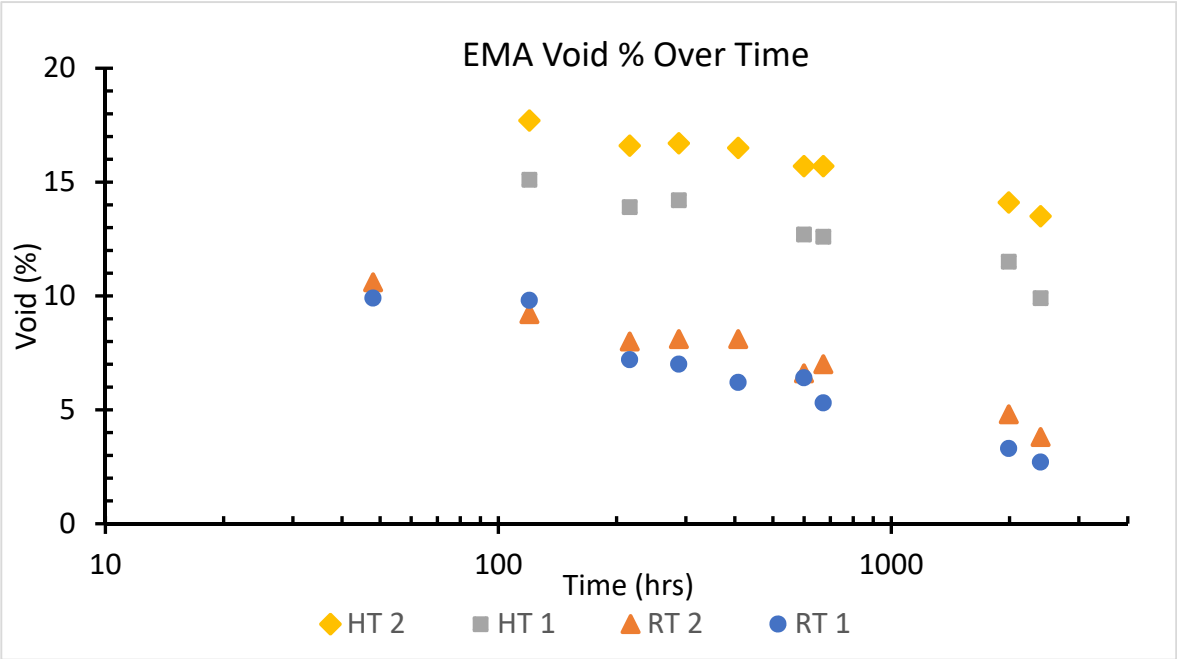


Figure 5. Void percentage of the sample as a function of time in oven. Note that each sample's void percentage decreases over time. This suggests that something may be filling the voids of films are becoming smoother with time.

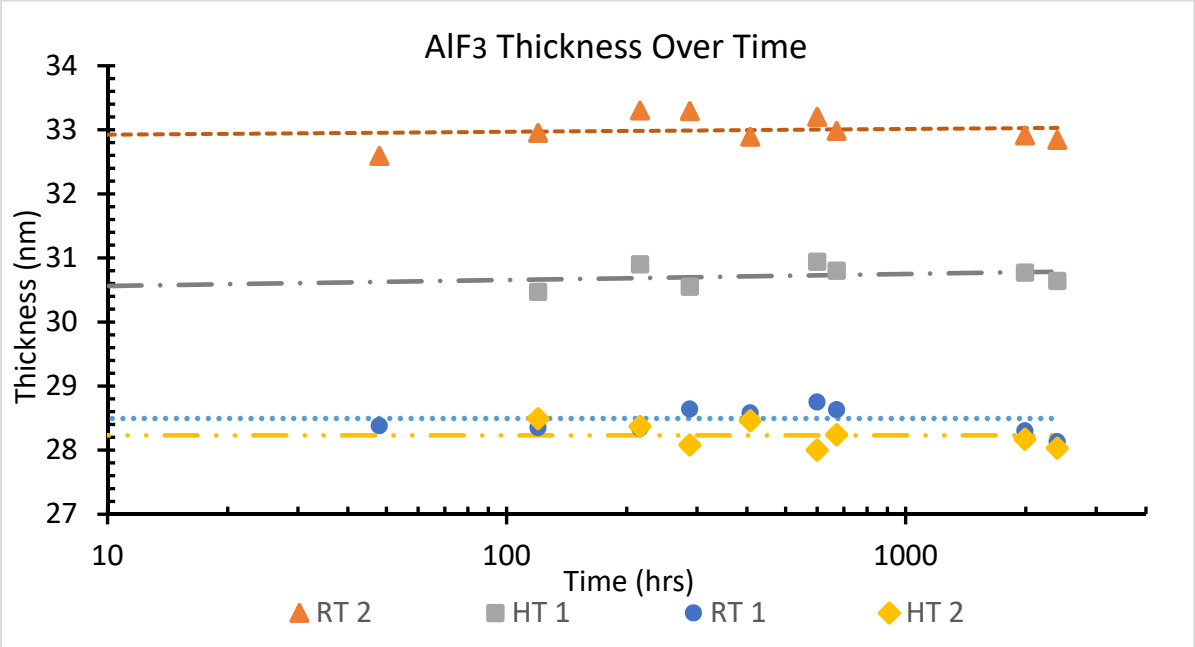


Figure 6. The apparent thickness of the AlF_3 capping layer for all four samples show negligible changes with time in oven. Here, RT denotes the two samples that were deposited on a room temperature substrate whereas HT denotes the other two samples that were deposited on a heated substrate. The logarithmic fits for each data set and the corresponding standard deviations are listed in Table 2.

Downloaded From: https://www.spiedigitallibrary.org/conference-proceedings-of-spie on 28 Dec 2022
Terms of Use: https://www.spiedigitallibrary.org/terms-of-use

Table 2. Best Logarithmic Fit Equations for Fig. 6. All samples from the final data set for each sample where fit to $y = Aln(t) + B$ where t is measured in hours. Notice that both RT 1 and HT 1 fit the coefficient A to zero, making the logarithmic fit a constant.

Sample	Best Logarithmic Fit	Standard Deviation (σ)
RT 1	$y = 28.49$	0.214
RT 2	$y = 0.0193\ln(t) + 32.88$	0.206
HT 1	$y = 0.0407\ln(t) + 30.47$	0.158
HT 2	$y = 28.23$	0.18

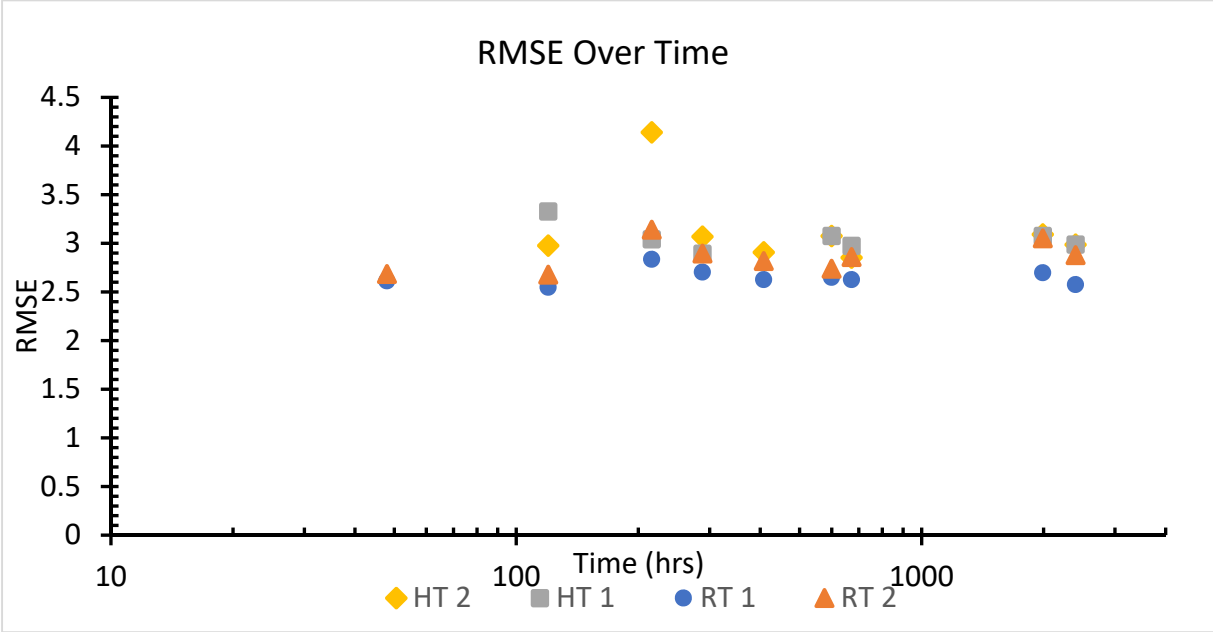


Figure 7. The RMSE value from fitting the ellipsometric data with the final optical model for each of the four sample as a function of oven time. Each data point represents the RMSE of the optical model's fit to the experimental ellipsometric data. All the R^2 values are reasonably low, and there is no strong trend in the value of the RMSEs with time.

Summarizing the results of modeling: Over the course of the 2500 hours of AlF_3 on Al samples stored in the 327K oven no significant changes in the thickness of the protective AlF_3 layer are observed via VASE. (See Fig. 6). The aluminum oxide thickness is small to begin with for all four samples and never increased over the 2500 hours for any of the samples. (Data not shown.) Insights in how to analyze SE data were also gained. SE data was modeled using a Bruggeman effective medium models and by optimizing layer parameters until an RMSE of about 3 was achieved. In the end, the most effective approach for modeling changes in the AlF_3 was to represent the layer as a two-component EMA material with AlF_3 and void as the primary and a secondary constituents, respectively. The void percentage that the model generated for each sample dropped by a factor of two by the end of the 2500 hours. However, excluding water completely from the EMA layer is probably not physical and should be re-examined.

Downloaded From: https://www.spiedigitallibrary.org/conference-proceedings-of-spie on 28 Dec 2022
Terms of Use: https://www.spiedigitallibrary.org/terms-of-use

4. SUMMARY AND CONCLUSIONS

Evaporated thin-film Al samples protected by thin (29±2 nm) AlF_3 overcoat stored in a 327 K environment over a period of 2500 hours exhibited no significant changes in the thicknesses of the protective AlF_3 layer as observed by variable-angled, spectroscopic ellipsometry. There were, however, changes in the ellipsometric psi and delta data with time that were interpreted as changes in void fraction. Using the fitting tool CompleteEASE, the ellipsometric data for the samples were analyzed using a two-component effective medium model and aluminum layer parameters were varied until an RMSE of approximately 3 was achieved. In the end, the final model for determining the change in the AlF_3 was represented as an EMA layer with AlF_3 and void, respectively as primary and a secondary constituents. Initial void percentages that the model calculated for each sample were roughly halved by the end of the 2500 hours in oven. Completely, excluding water in the EMA layer is probably not physical and should be re-examined. The disappearing void fraction suggests that the films might be becoming more compact with time. Initially it was thought that the AlF_3 was absorbing water and that accounted for the small amount of swelling seen in some models, but this idea was ruled out when the optical constants of Al and AlF_3 were optimized. In order to further understand the decrease in void percentage as well as the role of water, other methods such as AFM are needed to narrow down possible explanations for observed changes.

ACKNOWLEDGMENTS

Shania Chacon, Tyler Youngbull prepared the substrate heater used in depositing AlF_3 on hot surface. Joshua Vawdrey helped with early AFM work. Isaiah Galland and Raymond Kelly, Alex Gallion. We also gratefully acknowledge the financial support from BYU's College of Physical and Mathematical Sciences. We also gratefully acknowledge advice from James Hilfiker and other Woollam employees in modeling and in providing access to CompleteEASE on student computers.

REFERENCES

[1] Smith, D. Y., Shiles, E., Inokuti, M. and Palik, E. D., "The Optical Properties of Metallic Aluminum," [The Handbook of Optical Constants of Solids], E. D. Palik, Ed., Academic Press, Orlando, FL 32887, Florida, USA, 369–406 (1985).

[2] Fronk, K., "Storage of Al/AlF3 Thin-Film Mirrors in 327 K Oven" (2021).

[3] Hass, G., Hunter, W. R. and Tousey, R., "Reflectance of evaporated aluminum in the vacuum ultraviolet," J. Opt. Soc. Am. **46**(12), 1009–1012 (1956).

[4] Hass, G. and Tousey, R., "Reflecting coatings for the extreme ultraviolet," J. Opt. Soc. Am. **49**(6), 593–602 (1959).

[5] Canfield, L. R., Hass, G. and Waylonis, J. E., "Further studies on MgF_2-overcoated aluminum mirrors with highest reflectance in the vacuum ultraviolet," Appl. Opt. **5**(1), 45 (1966).

[6] Hunter, W. R., Osantowski, J. F. and Hass, G., "Reflectance of Aluminum Overcoated with MgF2 and LiF in the Wavelength Region from 1600 Å to 300 Å at Various Angles of Incidence," Appl. Opt. **10**(3), 540 (1971).

[7] Cox, J. T., Hass, G. and Waylonis, J. E., "Further Studies on LiF-Overcoated Aluminum Mirrors with Highest Reflectance in the Vacuum Ultraviolet," Appl. Opt. **7**(8), 1535 (1968).

[8] Lewis, D. M., Plewe, C. M., Stapley, A. G., Vawdrey, J. J., Turley, R. S. and Allred, D. D., "Illuminating the degradation of lithium fluoride mirror coatings in humid environments," Proc.SPIE **11451** (2020).

[9] Wilbrandt, S., Stenzel, O., Nakamura, H., Wulff-Molder, D., Duparré, A. and Kaiser, N., "Protected and enhanced aluminum mirrors for the VUV," Appl. Opt. **53**(4), A125--A130 (2014).

[10] Hennessy, J., Jewell, A. D., Balasubramanian, K. and Nikzad, S., "Ultraviolet optical properties of aluminum fluoride thin films deposited by atomic layer deposition," J. Vac. Sci. Technol. A **34**(1), 01A120 (2015).

[11] Moore, C. S., Hennessy, J., Kersgaard, E. and Jewell, A. D., "Current progress in the characterization of atomic layer deposited AlF3 for future astronomical ultraviolet mirror coatings.," Proc. SPIE, 1–15 (2015).

Downloaded From: https://www.spiedigitallibrary.org/conference-proceedings-of-spie on 28 Dec 2022
Terms of Use: https://www.spiedigitallibrary.org/terms-of-use

[12] Hutcheson, E. T., Hass, G. and Cox, J. T., "Effect of deposition rate and substrate temperature on vacuum ultraviolet reflectance of MgF2-overcoated and LiF-overcoated aluminum mirrors," Appl. Opt. **11**(10), 2245- (1972).

[13] Dauer, V., "Optical constants of lithium fluoride thin films in the far ultraviolet," J. Opt. Soc. Am. B **17**(2), 300–303 (2000).

[14] Quijada, M. A., Rice, S. and Mentzell, E., "Enhanced MgF2 and LiF over-coated Al mirrors for FUV space astronomy," Proc.SPIE **8450**, 84502H (2012).

[15] Rodríguez~De~Marcos, L. V, Larruquert, J. I., Méndez, J. A., Gutiérrez-Luna, N., Espinosa-Yáñez, L., Honrado-Benítez, C., Chavero-Royán, J. and Perea-Abarca, B., "Optimization of MgF2-deposition temperature for far UV Al mirrors," Opt. Express **26**(7), 9363–9372 (2018).

[16] Gutiérrez-Luna, N., Perea-Abarca, B., Espinosa-Yáñez, L., Honrado-Benítez, C., de Lis, T., Rodríguez-de Marcos, L. V., Aznárez, J. A. and Larruquert, J. I., "Temperature dependence of AlF3 protection on far-UV Al mirrors," Coatings **9**(7), 428 (2019).

[17] Balasubramanian, K., Hennessy, J., Raouf, N., Nikzaa, S., Ayala, M., Shaklan, S., Scowen, P., Hoyo, J. Del, Quijada, M. and Howard A. MacEwen, J. B. B., "Aluminum Mirror Coatings for UVOIR Telescope Optics including the Far UV," [UV/Optical/IR Space Telescopes and Instruments: Innovative Technologies and Concepts VII: Proc. of SPIE Vol. 9602], SPIE, Bellingham,, WA, 96020I-1–9 (2015).

[18] Hennessy, J., Balasubramanian, K., Moore, C. S., Jewell, A. D., Nikzad, S., France, K. and Quijada, M., "Performance and prospects of far ultraviolet aluminum mirrors protected by atomic layer deposition," J. Astron. Telesc. Instruments, Syst. **2**(4), 041206 (2016).

[19] Johnson, B. I., Avval, T. G., Turley, R. S., Linford, M. R. and Allred, D. D., "Oxidation of aluminum thin films protected by ultrathin MgF2 layers measured using spectroscopic ellipsometry and X-ray photoelectron spectroscopy," OSA Contin. **4**(3), 879–895 (2021).

[20] Li, X., Zhang, W., Sun, J., Liu, J., Hou, Y., Lin, L., He, K. and Yi, K., "Influence of oxygen pressure and substrate temperature on the properties of aluminum fluoride thin films," Appl. Surf. Sci. **282**, 226–230 (2013).

[21] Allred, D. D., Turley, R. S., Thomas, S., Willett, S., Perry, S. B. and Greenburg, M. J., "Adding EUV reflectance to aluminum mirrors for space-based observatories," UV/Optical/IR Sp. Telesc. Instruments Innov. Technol. Concepts VIII **10398**, H. A. MacEwen and J. B. Breckinridge, Eds., 10398Y, SPIE (2017).

[22] Miles, M., "Evaporated Aluminum Fluoride as a Barrier Layer to Retard Oxidation of Aluminum Mirrors" (2017).

[23] Johnson, B. I., Avval, T. G., Hodges, G. T., Carver, V., Membreno, K., Allred, D. D. and Linford, M. R., "Using ellipsometry and x-ray photoelectron spectroscopy for real-time monitoring of the oxidation of aluminum mirrors protected by ultrathin MgF2 layers," Proc.SPIE **11116**, 11116O (2019).

[24] Hilfiker, J. N., Singh, N., Tiwald, T., Convey, D., Smith, S. M., Baker, J. H. and Tompkins, H. G., "Survey of methods to characterize thin absorbing films with Spectroscopic Ellipsometry," Thin Solid Films **516**(22), 7979–7989 (2008).

[25] Herzinger, C. M., Johs, B., McGahan, W. A., Woollam, J. A. and Paulson, W., "Ellipsometric determination of optical constants for silicon and thermally grown silicon dioxide via a multi-sample, multi-wavelength, multi-angle investigation," J. Appl. Phys. **83**(6), 3323–3336 (1998).

[26] Rydalch, T. D., Lewis, D. M. and Allred, D. D., "Stability of lithium fluoride thin films as a function of humidity and temperature," Sp. Telesc. Instrum. 2022 Ultrav. to Gamma Ray, SPIE Proc. 12181, J.-W. A. den H. S. N. K. Nakazawa, Ed., SPIE-Intl Soc Optical Eng, Montreail (2022).

[27] Nguyen, H. V, An, I. and Collins, R. W., "Evolution of the optical functions of thin-film aluminum: A real-time spectroscopic ellipsometry study," Phys. Rev. B **47**(7), 3947 (1993).

[28] Johs, B. D., McGahan, W. A. and Woollam, J. A., "Optical analysis of complex multilayer structures using multiple data types," Thin Solid Films **253**(1–2), 25–27 (1994).

[29] McGahan, W. A., Johs, B. and Woollam, J. A., "Techniques for ellipsometric measurement of the thickness and optical constants of thin absorbing films," Thin Solid Films **234**(1–2), 443–446 (1993).

Downloaded From: https://www.spiedigitallibrary.org/conference-proceedings-of-spie on 28 Dec 2022
Terms of Use: https://www.spiedigitallibrary.org/terms-of-use